

Polybenzimidazole as a Promising Support for Metal Catalysis: Morphology and Molecular Accessibility in the Dry and Swollen State

A. A. D'Archivio,^[b] L. Galantini,^[b] A. Biffis,^[c] K. Jeřábek,^{*,[a]} and B. Corain^{*,[b,d]}

Abstract: Polybenzimidazole (PBI) in beaded form (250–500 μm) has been characterized in the dry state by scanning electron microscopy (SEM), BET, and nitrogen porosimetry. In the swollen state, it has been characterized by inverse steric exclusion chromatography (ISEC) in tetrahydrofuran, toluene, and water, by ESR of TEMPONE (2,2,6,6-

tetramethyl-4-oxo-1-oxypiperidine), and pulse field gradient spin echo (PGSE) NMR spectroscopy, toluene, in tetrahydrofuran, ethanol and water. The dry-state results are in good agreement

with the ISEC results obtained in tetrahydrofuran, toluene, and water with regard to the 40–80 nm macroporosity. The swelling-dependent surface area and pore volume detected by ISEC in toluene and water reveal the amphiphilic nature of PBI.

Keywords: catalysts • catalyst supports • polybenzimidazole beads

Introduction

Macromolecular cross-linked supports are widely used in synthesis and separations,^[1] in particular as catalysts for numerous industrial processes, the most important of which is the large-scale synthesis of methyl *tert*-butyl ether (MTBE) from methanol and isobutene (22.6 million tons in 1996).^[2a] In addition, they are used as active supports for palladium metal in the preparation of bifunctional catalysts comprising acid as well as hydrogenation-active centers. Such catalysts are employed, for example, in the industrial synthesis of methylisobutyl ketone (MIBK) (Bayer catalyst OC 1038),^[2c] where

the acid centers catalyze the dimerization of acetone to diacetone alcohol and its dehydration to mesityl oxide, which is then hydrogenated on the metal surface to the end product. Similar catalysts based on anion exchange resins (Bayer catalysts K 6333 and VP OC 1063)^[2c] are employed in industrial heat-exchange units for the reduction of dioxygen levels in water from ppm to ppb. Other applications include an alternative route to MTBE (EC Erdölchemie process)^[2a] and the etherification–hydrogenation of mixtures of unsaturated hydrocarbons to give blends of alkanes and branched ethers for the manufacture of unleaded petrol (BP Etherol Process).^[1a]

In comparison with their inorganic counterparts, synthetic functional resins offer much better control of the functionalization chemistry. Typically, their skeleton is composed of organic polymer chains interconnected by covalent cross-links and therefore insoluble in any solvent.^[1] In the dry materials, a detectable porosity can be observed only in so-called macroporous resins, polymerized in the presence of porogenic solvents, while the gel-type resins are glassy materials with no detectable porosity in the dry state. However, after absorption of suitable amounts of a liquid (either a solvent or a reactant) capable of effectively solvating the polymer chains, the swollen polymer network of both types exhibits an extensive microporosity, thus providing high capacity for supporting a variety of chemical functionalities.

Polybenzimidazole^[3] (PBI, Scheme 1) is a peculiar 'resin' in that its lack of solubility in many solvents is not due to covalent cross-links but to the structural rigidity of the polymer chains, and perhaps to the presence of interchain interactions through hydrogen bonds. PBI is particularly stable to thermoxidation (up to 600 °C), and is currently

[a] K. Jeřábek

Institute of Chemical Processes Fundamentals
Academy of Sciences of the Czech Republic
Rozvojova 135, 165 02 Suchbát, Praha 6 (Czech Republic)
Fax: (+42)2-20920661
E-mail: kjer@icpf.cas.cz

[b] B. Corain, A. A. D'Archivio, L. Galantini

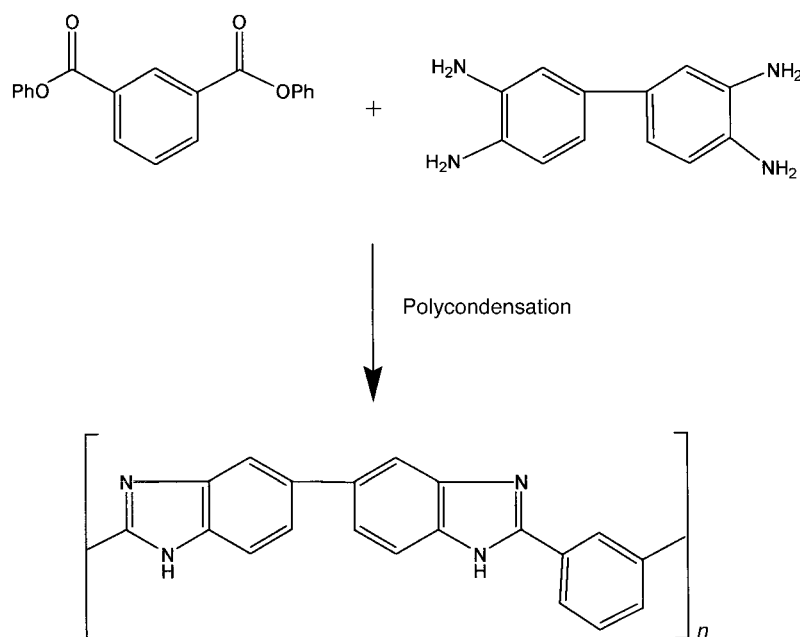
Dipartimento di Chimica, Ingegneria Chimica e Materiali
Università di L'Aquila
via Vetoio, Coppito Due, 67010 L'Aquila (Italy)
E-mail: corain@aquila.inf.it, anperuf@tin.it

[c] A. Biffis

Dipartimento di Chimica Inorganica Metallorganica e Analitica
Università di Padova
via Marzolo 1, 35131 Padova (Italy)

[d] B. Corain

Centro per lo Studio della Stabilità e Reattività dei Composti di Coordinazione, C.N.R.
c/o Dipartimento di Chimica Inorganica Metallorganica e Analitica
Università di Padova, 35131 Padova (Italy)
Fax: (+39)49-8275223



Scheme 1.

utilized in many high-temperature- and chemical-resistant applications such as flame-retardant applications and thermal-protective coatings. Other uses include the preparation of membranes for product separations and the application in

Abstract in Italian: *Polibenzimidazolo, in forma di sferule con diametro 250–500 μm e un grado di funzionalizzazione pari a 5.6 meq g^{-1} , viene caratterizzato allo stato secco tramite SEM, BET e porosimetria ad azoto, tramite cromatografia ISEC (inverse steric exclusion chromatography) allo stato rigonfiato in tetraidrofurano, toluene ed acqua, tramite la registrazione dello spettro ESR della sonda paramagnetica TEMPONE (2,2,6,6-tetrametil-4-ossio-1-ossipiperidina) in toluene tetraidrofurano, etanolo e acqua e tramite spettrometria PGSE-NMR in questa stessa terna di solventi. I risultati delle analisi eseguite nello stato secco concordano apprezzabilmente con i risultati ISEC ottenuti in tetraidrofurano, toluene ed acqua con specifico riferimento alla macroporosità di 40–80 nm. I valori di area superficiale e di porosità determinati tramite ISEC dopo rigonfiamento in toluene ed acqua, rivelano un carattere alquanto amfilifico del PBI.*

Abstract in Czech: *Perlový polybenzimidazol (průměr 250–500 μm ; stupeň funkcionalizace 5.6 meq g^{-1}) byl v suchém stavu charakterizován rastrovací elektronovou mikroskopií a adsorpcí dusíku. Ve zbotnalém stavu inverzní sterickou exkluzní chromatografií (ISEC) v prostředí tetrahydrofuranu, toluenu a ve vodě a dále pomocí ESR s TEMPONE (2,2,6,6-tetramethyl-4-oxo-1-oxypiperidin) a PGSE-NMR v toluenu, tetrahydrofuranu, ethanolu a ve vodě. Jak výsledky charakterizace v suchém stavu, tak i ISEC v tetrahydrofuranu, toluenu i vodě shodně indikovaly přítomnost makropórů o průměru 40 a 80 nm. Botáním rozvinutý specifický povrch a objem pórů detekovaný ISEC v toluenu a vodě ukazuje na poněkud amfilický charakter PBI.*

sorption technologies. With regard to the latter application, PBI can be manufactured as 250–500 μm beads with a certain degree of macroporosity (Hoechst-Celanese Corporation).

PBI has potential as a macromolecular ligand, capable of coordinating metal centers through its amino heteroatoms. To our knowledge, the first example of the metal coordination behavior of PBI (towards Pd^{II}) was described in 1985 by Li and Fréchet,^[4] who were interested in the utilization of this macromolecular metal complex as a precursor for a PBI-supported (metal) Pd catalyst. In recent years, considerable work has been carried out by Sherrington and co-workers, who employed PBI to anchor, inter alia, the unit $[\text{MoO}_2(\text{acac})]$ (acac = acetylacetonate), to give a very efficient, selective and reusable ‘hybrid phase’^[5] catalyst for

the epoxidation of technologically relevant alkenes.^[6]

Despite the growing field of application of PBI and the potential of this material as a mechanically, hydrolytically and thermooxidatively stable polymer support in catalysis, little is known about its textural properties in terms of macro-, meso-, and microporosity. Recently, molecular structural and morphological characterization of PBI and PBI-supported Mo^{VI} alkene epoxidation catalysts were investigated by a number of instrumental methods.^[7] However, this study was performed on dry samples only. Polymer supports and catalysts are usually applied in liquid media, in which due to swelling their morphology and the accessibility of their supported functionality is different from that seen in the dry state. The characterization of the macromolecular environment inside the swollen polymer networks of catalytically relevant resins is of particular interest,^[8–11] and we have investigated textural properties of beaded PBI from Hoechst-Celanese (i.e. the same material as that used in references [5] and [6]) in various solvents. This investigation has been performed by using inverse steric exclusion chromatography (ISEC), ESR, and pulse field gradient spin echo NMR (PGSE-NMR) spectroscopy of the material in various liquid media. In order to gather visual information on the morphology (albeit about a dried material), we have also performed a thorough scanning electron microscopy (SEM) analysis.

Results and Discussion

The morphology of dry PBI as shown by SEM resembles that of a solid foam (Figure 1). Pores appear as spherical and cylindrical cavities surrounded by relatively thin polymer walls. In contrast with the pore formation in conventional macroporous polymer supports, for example the copolymers of styrene-divinylbenzene^[1] (where the polymer phase forms

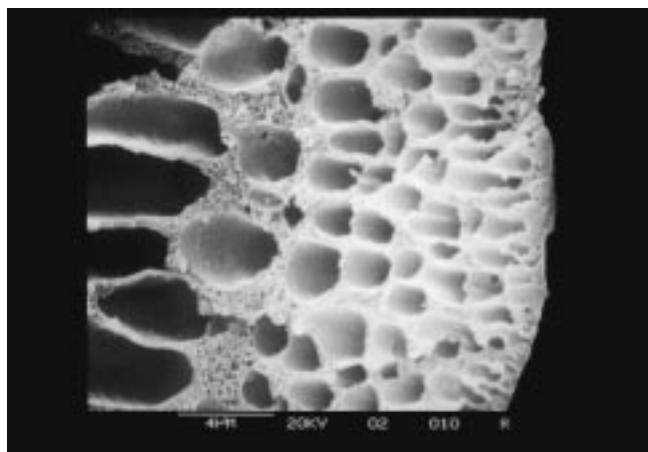


Figure 1. SEM image of the interior of a PBI bead.

microspheres surrounded by the liquid porogen), in the pore-forming phase-separation occurring in PBI the porogenic liquid forms spherical drops surrounded by a polymer membrane.

Dry PBI appears to be an exceptionally porous material with a number of pores with diameters ranging from a few microns down to a few hundred nm. Although the porosity revealed by SEM appears to be impressive, the pores visible in Figure 1 are not particularly significant for the function of PBI as a support. In fact, pores of these sizes can provide only a small specific surface area, which has been confirmed by the quantitative evaluation of the dry-state porosity by nitrogen porosimetry. This technique reveals a total pore volume equal to $0.11 \text{ cm}^3 \text{ g}^{-1}$ with a mean pore diameter equal to 40 nm and a cumulative surface area of $12 \text{ m}^2 \text{ g}^{-1}$. The t-plot analysis indicates the presence of a small number of micropores responsible for an additional $10 \text{ m}^2 \text{ g}^{-1}$ of surface area. This dry-state morphology quantitative feature fits nicely the BET surface area value of $20 \text{ m}^2 \text{ g}^{-1}$.

ISEC^[12, 13] allows access to information on the swollen-state morphology of polymeric materials, which, with regard to the working state of the polymer support, is much more relevant than the data obtained by conventional methods on dry materials. The method is based on the measurements of elution volumes of standard solutes of known molecular sizes running through a chromatographic column filled with resins to be evaluated in terms of their textural features. Our measurements were performed alternatively with THF, toluene, and aqueous mobile phases, to get information on the swollen-state morphology in the solvents in which the ESR and PGSE-NMR measurements were also performed.

ISEC results show that in toluene PBI swells substantially less than in THF. The volume of the swollen polymer particles is found to be 3.68 mL g^{-1} in THF, while in toluene it turns out to be only 2.33 mL g^{-1} . This is computed as the inner column volume (4.04 mL) minus the dead volume, divided by the weight of the sample. The measurements in water were very

difficult. The peaks of the standard solutes (deuterium oxide, sugars, and dextrans) were rather broad with an evident tailing. In measurements carried out with our usual aqueous mobile phase (0.2 M sodium sulfate), most of the dextrane solutes could not be eluted from the column at all. We have already observed this phenomenon and found that a possible remedy is to saturate the surface of the examined resin with a dextrane (achieved upon utilizing a mobile phase containing a dextrane admixture). Solute injected during ISEC experiments are then no longer adsorbed, and their elution behavior better corresponds to steric effects only. ISEC measurements carried out with the aqueous mobile phase containing sodium sulfate and 0.5% dextrane (MW 6000) gave reasonable results, and the overall textural picture deduced from the measurements in water appears to be similar to that observed in toluene.

In principle, macroporous resins possess pores of two types: the so-called 'true pores', that is holes between domains of swollen polymer mass, and the spaces between polymer chains in the swollen polymer gel matrix.^[1]

Pores with an effective diameter greater than about 10 nm are too large to be considered as a part of swollen polymer mass, and can be unambiguously assigned to the macropore (or 'true pore') category and depicted in terms of a cylindrical pore model.^[13] Data relevant to this part of the swollen PBI morphology are collected in Table 1.

The widest pores, which in THF (the best swelling solvent) are characterized by an effective diameter of 80 nm and in toluene and water one of 40 nm, are likely to be the pores

Table 1. Macroporous features of PBI detected by ISEC.

Solvent	Pore diameter = 80 nm		Pore diameter = 40 nm		Pore diameter = 10–20 nm	
	pore volume [$\text{cm}^3 \text{ g}^{-1}$]	surface area [$\text{m}^2 \text{ g}^{-1}$]	pore volume [$\text{cm}^3 \text{ g}^{-1}$]	surface area [$\text{m}^2 \text{ g}^{-1}$]	pore volume [$\text{cm}^3 \text{ g}^{-1}$]	surface area [$\text{m}^2 \text{ g}^{-1}$]
THF	0.29	14.7	0	0	2.25	643
toluene	0	0	0.08	8	1.30	384
water	0	0	0.15	15	1.02	227

detected by SEM and nitrogen porosimetry in the dry material (Figure 2). However, the most prominent part of the swollen-state porosity are the pores with the diameter 10–20 nm, evidently generated by the swelling process in all three solvents employed. They offer much greater capacity for supporting a functionality than the pores detectable in the dry state, and their existence is likely to explain the observed excellent catalytic properties of PBI as a support for Mo^{VI} hybrid phase catalysts.^[6] The detected pore volume (in THF $2.25 \text{ cm}^3 \text{ g}^{-1}$) corresponds to an extremely high porosity, around 75% (if we consider the density of the PBI polymer matrix to be about 1.3 g cm^{-3} [3]). Such high porosity is possible only thanks to the foamy morphology of PBI (as revealed by SEM). In a material with pores created as spaces between microparticles^[1] (e.g. conventional macroporous resins), the porosity is at most 40–50%.

In macroporous resins, the pores smaller than 10 nm can be interpreted, in principle, either as 'true pores', that is cylindrical holes, or as the porosity of swollen polymer gel, that is as spaces between randomly oriented cylindrical rods

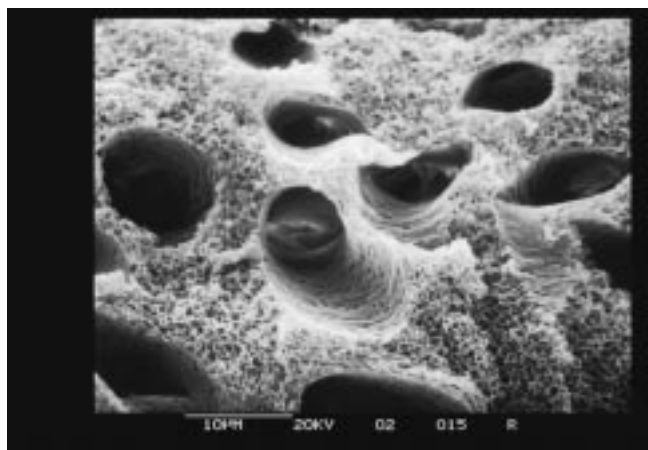


Figure 2. Hierarchy of pores in PBI. SEM image of an internal fragment of a PBI bead showing a group of large macropores surrounded by resin domains featured by an array of smaller macropores.

representing the polymer chains (Ogston's model^[14]). From the mathematical point of view both models are equivalent and the best depiction must be selected on the basis of additional indications. ISEC-derived data on the meso- and microporosity of solvent-swollen PBI is shown in Table 2. Micropores with molecular dimensions attributable with certainty to the swollen polymer mass were detected only in PBI swollen by THF. In the terms of Ogston's model these pores are characterized by a polymer chain concentration equal to 2 nm^{-3} , which corresponds to a rather dense, poorly swollen polymer mass. In toluene and water these micropores were not detected and this indicates negligible swelling of PBI polymer mass in these media. Yet, the ISEC measurements in all three solvents also indicated the existence of another category of pores that in the Ogston model would be characterized by the polymer chain concentration 0.4 nm^{-3} . Such polymer chain concentration would represent a rather highly swollen polymer network, and it is difficult to imagine that such swollen polymer fractions would be characterized in all three different solvents by the same polymer chain concentration. Therefore, we felt it more appropriate to describe this pore fraction as cylindrical mesopores with the effective diameter 3 nm (second column in Table 2).

The ISEC data suggest that the foamlike morphology clearly exhibited by SEM is a cascade of smaller and smaller pores. Two levels of this pore distribution are illustrated in Figure 2. ISEC analysis shows that the volume increase after treating dry PBI with a solvent is not in fact the result of actual swelling of the polymer mass, but rather a restoration or regeneration of the 'true pores', which collapsed during drying. As the result, all supported functionality turns out to

be accessible through macro-, and mesopores. The volume of the porous domains is relatively unaffected by the type of solvent, and this suggests that the pore restoration is probably aided by a strain created in the rigid polymer by pore collapse during drying. Structural rigidity of the PBI polymer chains is attributed to multiple interchain interactions through hydrogen bonds. It evidently produces an effect similar to that observed in the hypercrosslinked resins developed by Davankov and Tsyurupa.^[15]

ESR: ESR analysis based on the dispersion of TEMPONE inside swollen PBI reveals that the rotational motion of the paramagnetic probe is affected by the nature of the swelling medium. The ESR spectra of swollen PBI in THF and EtOH consist of sharp triplets typical of nitroxide spin-probes in the fast-motional regime,^[16] whereas in water and in toluene, a broad signal due to a slow rotational motion also contributes (Figure 3).

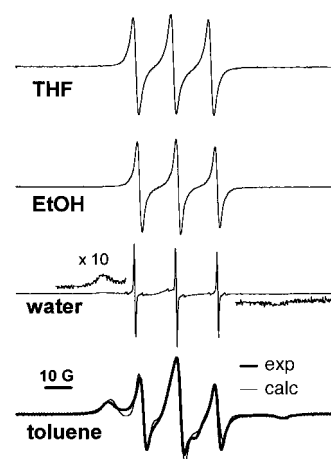


Figure 3. ESR spectra of solutions of TEMPONE confined inside PBI

In THF-, EtOH- and water-swollen PBI, the correlation time of the fast motion τ_{fast} is calculated from the spectral features of the sharp lines. However, the value in water only approximately describes the fast rotational motion because of its superposition with the broad signal. We obtain $\tau_{\text{fast}} = 4.7 \times 10^{-11}$, 1.3×10^{-10} , and 2.6×10^{-11} s, for THF-, EtOH-, and water-swollen PBI, respectively, which, if compared with the values in pure solvents (1.6×10^{-11} , 1.6×10^{-11} , and 1.3×10^{-11} s) suggests that the spin-probe responsible for the fast-motion spectral signal rotates inside relatively large pores, or gel volumes with low polymer chain concentration.^[8, 11] On the basis of computer simulation, the 'slow' contribution in toluene-swollen PBI is estimated to be about 20%, and the 'slow' and 'fast' rotational correlation times are calculated to be 1.7×10^{-8} s and 1.7×10^{-11} s, respectively. Again, τ_{fast} is comparable with the correlation time in bulk solvent (8.0×10^{-12} s). On the other hand, the 'slow' contribution originates from a non-negligible fraction of the TEMPONE

Table 2. Meso- and micropores in PBI swollen in three different solvents.

Solvent	Mesopores, pore diameter = 3 nm pore volume [$\text{cm}^3 \text{g}^{-1}$]	Swollen gel, chain concentration = 2 nm^{-3} swollen gel volume [$\text{cm}^3 \text{g}^{-1}$]
THF	0.37	0.19
toluene	0.31	0
water	0.78	0

molecules which are strongly immobilized. The observed hindrance of the rotational motion may be due to the dispersion of the spin-probe inside denser gel volumes, or to enthalpic interactions of TEMPONE with the polymer leading to partial adsorption of the spin probe onto the polymer chains. To examine this point, experiments were carried out using TEMPONE as ISEC probe. The effective diameter of the TEMPONE molecule is about 0.64 nm.^[17] In the absence of nonsteric interactions, its elution volume should be close to that of heptane (effective diameter 0.63 nm) or between the elution volumes of ribose and xylose (effective diameter 0.57 nm and 0.78 nm, respectively). In view of the lack of significant denser gel-type volumes revealed by ISEC analysis, the second hypothesis appears to be plausible and compatible with the observed higher surface area of toluene-swollen PBI. The elution volume of TEMPONE in THF is 3.30 mL, slightly higher than the elution volume of pentane (3.14 mL). The elution volume of heptane under the same conditions is 3.07 mL. Therefore, the adsorption of TEMPONE onto the resin from THF albeit not negligible, is apparently rather weak. In toluene, the elution volume is found to be greater than 6.3 mL, which is considered as strong evidence for very strong, practically irreversible, adsorption. As described above, in water most of the standard probes used in ISEC measurements are heavily adsorbed by PBI, and in order to contrast this adsorption it was necessary to employ a mobile phase containing 0.5% of dextrane (MW 6000). In the absence of dextrane, TEMPONE also undergoes strong adsorption.

PGSE-NMR: PGSE-NMR analysis reveals a single-component translational diffusion^[18] of the solvent molecules in THF-, EtOH-, and water-swollen PBI (Figure 4).

The self-diffusion coefficients D of THF, EtOH, and water in swollen PBI are shown in Table 3, compared with the self-

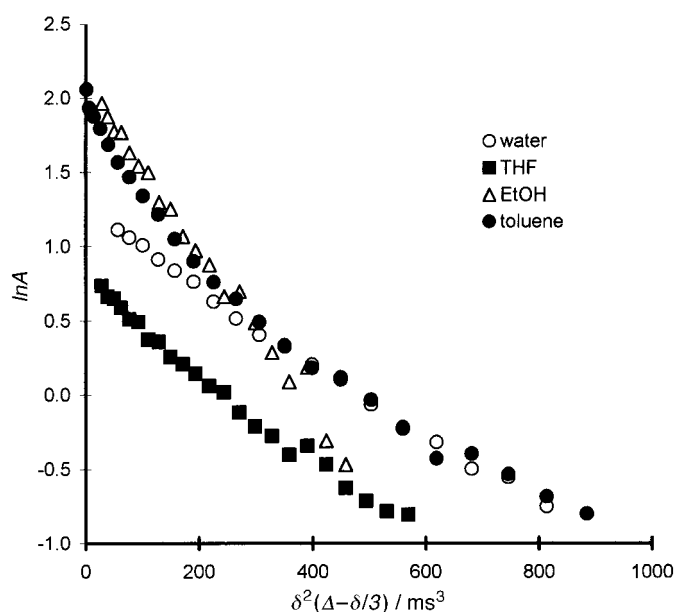


Figure 4. Echo's amplitude of PGSE signals in various solvents after swelling of PBI particles (see text).

Table 3. Solvent mobility data provided by PGSE-NMR analysis inside swollen PBI.

Swelling medium	D [cm^2s^{-1}]	E_a [kJ mol^{-1}]	D_0 [cm^2s^{-1}]	E_a [kJ mol^{-1}]
water	1.56×10^{-5}	18 ± 1	2.23×10^{-5}	18 ± 1
ethanol	7.51×10^{-6}	14 ± 1	1.08×10^{-5}	13 ± 1
THF	1.50×10^{-5}	10 ± 1	2.48×10^{-5}	8 ± 1

diffusion coefficients of the pure solvent D_0 . The activation energy values of the diffusion process (E_a), calculated from Arrhenius plots in the temperature range 5–35 °C, are also reported (again, the suffix 0 refers to the pure solvent). The invariance of the activation energy in the swollen PBI and in bulk medium is consistent with a viscosity-controlled diffusion process. The moderate reduction of D indicates that the movement of the solvent molecules is relatively free and likely controlled by the microviscosity of the medium which is only slightly affected by the presence of the polymer.

PGSE-NMR analysis in toluene-swollen PBI implies the coexistence of solvent molecules with different self-diffusion coefficients, which are not able to exchange efficiently within the time scale of the spin-echo experiment. In this specific case, further investigation is apparently needed.

Conclusion

PBI in beaded form combines thermal, hydrolytic and thermooxidative stability, as well as mechanical robustness with exceptional textural properties. Both porosity and surface area grow markedly after contact with liquids. This porosity development is assisted by a stress created in the backbone by the collapse during drying, rather than by a swelling of the polymer mass, and is not particularly dependent on the nature of the solvent. It promotes an expectation that PBI is a plausible support candidate for operating in diverse liquid media. Moreover, its chemical functionality makes PBI a promising macromolecular ligand suitable for metalation with a variety of metal centers, to give catalytically interesting macromolecular complexes useful per se or as precursors of catalytically active nanocrystallites.

Experimental Section

General methods: Solvents and chemicals were of reagent grade. TEMPONE was from Aldrich and was used as received. PBI, in beaded form, 250–500 μm , with a ligand content equal to 5.6 meq g^{-1} , was from Hoechst–Celanese and was purified as reported in references [5] and [6].

Nitrogen porosimetry: The measurements and data evaluation were performed using ASAP 2010 apparatus with dedicated software (Micromeritics, USA). BET surface area was determined from the adsorption data collected in the range of relative pressures 0.06–0.25. Cumulative surface area, pore volume, and medium pore diameter were evaluated from the desorption data on the basis of BJH theory.

ISEC: This analytical technology was employed for the characterization of the swollen-state morphology of PBI. The measurements were carried out using an established procedure and a standard chromatographic set-up described elsewhere.^[12, 13]

ESR: About 0.25 g of material was swollen with a nitrogen-saturated (10^{-4}M) solution of the paramagnetic probe TEMPONE (2,2,6,6-tetra-

methyl-4-oxo-1-oxypiperidine). The samples were allowed to reach the swelling equilibrium, the excess solution was removed by pouring the suspension obtained onto filter paper, and the swollen material was then rapidly transferred into the ESR tube. The ESR spectra were recorded at 293 K on an X-band JEOL JES-RE1X apparatus at 9.2 GHz (modulation 100 kHz). The rotational correlation time τ of TEMPONE in the fast-rotational spectra was calculated according to the Equation (1),^[19, 20] where

$$\tau = 6.14 \times 10^{-10} \Delta H_0 [(h_0/h_{+1})^{1/2} + (h_0/h_{-1})^{1/2} - 2][1 - 1/5(1 + \omega_e^2 \tau^2)] \quad (1)$$

$\omega_e = 5.78 \times 10^{10}$ Hz; the parameters h_{+1} , h_0 and h_{-1} (the intensities of the low-, middle-, and high-field lines, respectively) and ΔH_0 (the peak–peak width of the central line) were obtained directly from the double-derivative spectrum by peak-picking. The τ values in two-component spectra are evaluated by a nonlinear least-squares fits to experimental spectra. A Brownian isotropic model for the rotational diffusion was assumed and the fitting procedure was carried out by using the program NLSL.^[21] Published values for the anisotropic g and A tensors for TEMPONE^[22] are used in computation and spectra simulation.

PGSE-NMR: The self-diffusion coefficients of the swelling solvents were determined by ¹H-pulsed-gradient-spin-echo nuclear magnetic resonance (PGSE-NMR) measurements.^[18] In this technique a spin-echo experiment is performed while two magnetic field gradient pulses of magnitude G , duration δ and separation Δ are applied during the dephasing and the rephasing period, respectively. In the present study the interval Δ between the magnetic field gradient pulses was kept constant and equal to the interval t between the 90°–180° radio frequency pulses. Under these conditions, for a nucleus with diffusion coefficient D , the height of the echo amplitude A is given by Equation (2), where γ is the magnetogyric ratio and

$$A = A_0 \exp[-2t/T_2 - \gamma^2 G^2 D^2 \delta^2 (\Delta - \delta/3)] \quad (2)$$

T_2 is the spin spin relaxation time of the nucleus. In the typical experiment A was measured at $\Delta = 20$ ms and $G = 17.5$ G cm⁻¹ by varying δ up to 6 ms. The gradient strength was calibrated to values of the self-diffusion coefficient of pure water. The chosen t value was sufficient to remove the polymer contribution from the echo signal due to the relatively short T_2 relaxation time of the polymer hydrogens. The solvent diffusion coefficient was obtained from the slope of the logarithmic plot of A versus the term $\delta^2(\Delta - \delta/3)$. The samples were prepared as described above after swelling in the appropriate solvent and then placed in a 5 mm NMR tube. The spectra were recorded on a Bruker SXP 4-100 MHz apparatus operating at 21 MHz for protons, over the temperature range 5–35 °C at 5° intervals. The temperature of the sample during the measurements was controlled by a variable temperature unit BRUKER-VT 100 to an accuracy of within ± 0.25 °C.

Acknowledgements

We are grateful to Professor D. C. Sherrington for helpful discussion and for providing a generous sample of PBI from Hoechst–Celanese. The work described in this paper has been carried out during a visit of B. C. to the Institut für Organische Chemie und Biochemie, TU München. B. C. is grateful to the Alexander von Humboldt Foundation for a 'Wiederaufnahme' scholarship. This work was supported in part by Grant No. 104/99/0125 from the Grant Agency of the Czech Republic.

- [1] a) D. Sherrington, *Chem. Commun.* **1998**, 2275–2286; b) A. Guyot, *Pure Appl. Chem.* **1988**, *60*, 365–376.; c) A. Guyot in *Synthesis and Separations using Functional Polymer* (Eds: D. C. Sherrington, P. Hodge), Wiley, New York, **1988**, pp. 1–42.
- [2] a) P. M. Lange, F. Martinola, S. Oeckel, *Hydrocarbon Processing*, **1985**, *64*(12), 51–52; b) A. Mitschker, R. Wagner, P. M. Lange in *Heterogeneous Catalysis and Fine Chemicals* (Eds.: M. Guisnet, J. Barbier, J. Barrault, C. Bouchoule, D. Duprez, G. Pérot, C. Montassier), Elsevier, Amsterdam, **1988**, pp. 61–73; c) R. Wagner, P. M. Lange, *Erdöl, Erdgas, Kohle* **1989**, *105*, 414–419; d) K. Weissermerl, H. J. Arpe, *Industrial Organic Chemistry*, 3rd ed., VCH, Weinheim, Germany, **1997**, p. 71.
- [3] *Encyclopedia of Polymer Science and Engineering*, Vol. 11, Wiley, New York, **1988**, pp. 572–601.
- [4] a) N. H. Li, J. M. J. Fréchet, *J. Chem. Soc. Chem. Commun.* **1985**, 1100–1110; b) N. H. Li, J. M. J. Fréchet, *React. Polym.* **1987**, *6*, 311–321.
- [5] R. H. Grubbs, *CHEMTECH* **1977**, *7*, 512.
- [6] a) M. M. Miller, D. C. Sherrington, S. Simpson, *J. Chem. Soc. Perkin Trans.* **1994**, *2*, 2091–2096; b) M. M. Miller, D. C. Sherrington, *J. Catal.* **1995**, *152*, 368–376; c) M. M. Miller, D. C. Sherrington, *J. Catal.* **1995**, *152*, 377–383.
- [7] S. Leinonen, D. C. Sherrington, A. Snedon, D. McLoughlin, J. Corker, C. Canevali, F. Morazzoni, J. Reedijk, S. B. D. Spratt, *J. Catal.* **1999**, *183*, 251–266.
- [8] A. Biffis, B. Corain, M. Zecca, C. Corvaja, K. Jeřábek, *J. Am. Chem. Soc.* **1995**, *117*, 1603–1606.
- [9] M. Zecca, A. Biffis, G. Palma, C. Corvaja, S. Lora, K. Jeřábek, B. Corain, *Macromolecules* **1996**, *29*, 4655–4661.
- [10] B. Corain, K. Jeřábek, *Chim. Ind. Milan* **1996**, *78*, 563–567.
- [11] A. D'Archivio, L. Galantini, A. Panatta, E. Tettamenti, B. Corain, *J. Phys. Chem. B* **1998**, *102*, 6774–6779.
- [12] K. Jeřábek, *Anal. Chem.* **1985**, *57*, 1598–1602.
- [13] K. Jeřábek in *Cross Evaluation of Strategies in Size-Exclusion Chromatography*, ACS Symposium Series 635 (Eds.: M. Potschka, P. L. Dubin), American Chemical Society, Washington DC, USA, **1996**, pp. 211–224.
- [14] G. Ogston, *Trans. Faraday Soc.* **1958**, *54*, 1754–1757.
- [15] V. A. Davankov, M. P. Tsyurupa, *React. Polym.* **1990**, *13*, 27–42.
- [16] P. L. Nordio in *Spin Labeling-Theory and Applications*, Vol. 1 (Ed. L. J. Berliner), Academic Press, New York, **1976**, pp. 5–52.
- [17] J. S. Hwang, R. P. Mason, L. P. Hwang, J. H. Freed, *J. Phys. Chem.* **1975**, *79*, 489–511.
- [18] a) P. Stilbs, *Prog. NMR Spect.* **1987**, *19*, 1–45, and references therein; b) S. Pickup, F. D. Blum, W. T. Ford, M. Periyasamy, *J. Am. Chem. Soc.* **1986**, *108*, 3987–3990.
- [19] D. B. Chestnut, J. F. Hower, *J. Phys. Chem.* **1971**, *75*, 907–912.
- [20] M. F. Ottaviani, *J. Phys. Chem.* **1987**, *91*, 779–784.
- [21] D. E. Budil, S. Lee, S. Saxena, J. H. Freed, *J. Magn. Reson. A* **1996**, *120*, 155–189.
- [22] M. Brustolon, A. L. Maniero, C. Corvaja, *Mol. Phys.* **1984**, *51*, 1269–1281.

Received: March 26, 1999 [F 1701]